Program Digest, 2019 IEEE International Ultrasonics Symposium (IUS)
Glasgow, Scotland, October 6-9, 2019

Real-time contrast-enhanced ultrasound imaging using pulse inversion spectral deconvolution

Mawia Khairalseed [1,2], Kenneth Hoyt [1*]
Department of Bioengineering, University of Texas at Dallas, Richardson, TX, USA[1]
Department of Biomedical Engineering, Sudan University of Science and Technology
and Africa City of Technology, Khartoum, Sudan [2]
[*] kenneth.hoyt@utdallas.edu

***Abstract*—Contrast-enhanced ultrasound (CEUS) involves the use of a microbubbles (MB) contrast agent and specialized ultrasound (US) imaging techniques. Any progress that can improve image quality and contrast, could positively impact patient management. Herein we introduce the concept of nonlinear filtering of backscattered US data for separating the tissue and MB signal components. Termed pulse inversion spectral deconvolution (PISD), this method does not require multiple pulse transmissions, which is typical for many nonlinear US imaging modes. Our new PISD-based CEUS approach uses two Gaussian-weighted Hermite polynomials (GH) to form two inverted pulse sequences. The two inverted pulses are then used to filter US backscattered data and discrimination of the linear and nonlinear signal components. A programmable US scanner (Vantage 256, Verasonics Inc) equipped with a linear array transducer was implemented with real-time PISD-based CEUS imaging. The receive data from all channels were shaped using plane wave imaging beamforming with angular compounding (1 to 9 angles). *In vitro* data was collected using a tissue-mimicking flow phantom perfused with a MB contrast agent (Definity, Lantheus Medical Imaging) using both PISD and traditional nonlinear US imaging as comparison. Contrast enhancement was quantified by computing the contrast-to-tissue ratio (CTR). Preliminary *in vivo* data was collected in the hindlimb of a healthy mouse. These *in vitro* and *in vivo* results collectively show that PISD-based CEUS imaging yields improved image contrast compared to the more traditional nonlinear US imaging approach.**

Keywords—Angular compounding; microbubbles; plane waves; pulse-inversion spectral deconvolution; ultrasound imaging.

I. Introduction

Ultrasound (US) contrast agents (UCAs) are a class of diagnostic reagents that are usually gas-filled microbubbles (MBs) with a diameter in the range of 1 to 10 μm [1]. UCAs are excellent intravascular tracers and have been used clinically for several decades now [2]–[6]. Contrast-enhanced US (CEUS) imaging has generated increased attention in recent years due in part to FDA approval of a commercial UCA for use in liver imaging and characterization of focal liver lesions in adult and pediatric patients. The expanded indication of this contrast agent will likely serve as a catalyst for increased clinical and off-label use of these MBs.

Contrast agents improve contrast between blood and tissue because of their high nonlinearity under a low mechanical index (MI). To better detect the nonlinear backscattered US signal from the MBs, several CEUS imaging sequences are used to suppress the linear tissue signals [7], [8]. When using a harmonic-based nonlinear (NLI) imaging method, the following problem is always met. If a US pulse is transmitted, there is an expected spectral overlay between the harmonic and central frequencies. Transmitting with a longer US pulse (narrowband) improves detection of the harmonic signals from insonated MBs, but compromises imaging resolution [9], [10]. To improve the trade-off between image resolution and contrast, several different CEUS imaging techniques have been developed that rely on exciting MBs with multiple transmission events (i.e. pulse-echo events). The emitted pulse of the second or third transmission event is generated by modifying the pulse polarity [11], [12], amplitude [13], or both [14]–[16].

Herein we present the concept of nonlinear filtering of backscattered US data for separating the linear and nonlinear US signal components. Termed pulse inversion spectral deconvolution (PISD), this method does not need multiple pulse transmissions, which is typical for many nonlinear CEUS imaging modes noted above. Like the multiple pulse-based NLI imaging methods, PISD does not require band-limiting the transmit pulses to simplify the separation of the linear and nonlinear components. That is, PISD can be designed to extract nonlinear echo components throughout the spectrum of the echo data, not just at the expected bands (e.g. harmonic or subharmonic frequencies). This approach allows the use of standard US imaging pulses designed to provide the best possible resolution and signal-to-noise ratio (SNR) while utilizing the full bandwidth of the US imaging transducer.

II. Methodology

A. Ultrasound Imaging

US data for PISD and NLI (for comparison) were acquired using a Vantage 256 programmable scanner equipped with a 128-element L11-4v linear array transducer (Verasonics Inc, Kirkland, WA). This system contains a 12-core processing unit

This work was supported in part by National Institutes of Health (NIH) grants K25EB017222, R21CA212851, and R01EB025841 and Cancer Prevention Research Institute of Texas (CPRIT) award RP180670.

and 132 GB of memory (RAM). Plane wave imaging (PWI) was performed at a center frequency of 4.5 MHz and the received data from all array elements (channels) was formed using PWI beamforming. Backscattered US data was sampled at a rate equal to 4x the center frequency and quantized at 12 bits. A low MI was used to minimize UCA destruction and to assess the impact of US pulse pressure on image quality (MI = 0.1, 0.2 or 0.3). These values were confirmed by physical measurements using a hydrophone system (AIMS III, Onda Corp, Sunnyvale, CA). All US data was collected at a frame rate of 30 Hz and depth of 15 mm. Traditional NLI imaging was performed after implementing the classic contrast pulse sequencing method [17]. CEUS imaging using a single plane wave (N = 1 angle) was compared to results following beam steering (in range of -18 to 18 degrees) and angular compounding (N = 5 or 9 angles).

B. Pulse Inversion Spectral Deconvolution (PISD)

Gaussian-weighted Hermite polynomials (GWHP) are linked to the physics of scattering within a standard model of pulse-echo US systems [18]–[20]. A pair of GWHP functions, $GH_2(t)$ and $GH_7(t)$, were used to form two filtering kernels, namely, $e_1(t)$ and $e_2(t)$. These two pulses were then used as parallel convolution filters and applied to the backscattered US data to measure the amplitude of the received signals relative to $e_1(t)$ and $e_2(t)$. The signal envelope for each of these filtered data sequences was then calculated using a Hilbert transformation. The images were formed using pixel-based image reconstruction [21]–[23]. All PISD processing was done on each RF image plane before averaging to get the angular compounded image. The dynamic range of both PISD and NLI images was 8-bit. A schematic diagram of the PISD method and display of the CEUS image is summarized in Fig. 1.

C. In Vitro Data

An experimental setup involved a tissue-mimicking vascular flow phantom (Model 524, ATS Labs Bridgeport CT) and peristaltic pump (L/S Digital Console Pump System, Cole-Parmer, Vernon Hills, IL) connected to a stirred water reservoir via silicon tubing. The flow phantom vessel internal diameter was 4 mm and located at a fixed depth of 15 mm below the scan surface. The US attenuation coefficient of the surrounding solid material was reported by the manufacturer to be 0.5 dB/cm/MHz. An UCA (100 µL) was introduced to the mixing reservoir (Definity, Lantheus Medical Imaging, N Billerica, MA) and circulated through the flow phantom at a rate of 110 mL/min. This rate is similar to the very slow flow in microvascular networks (about 1 to 5 mm/sec). With the transducer fixed in either a longitudinal or transverse position over the vessel, both PISD and NLI imaging was performed.

D. In Vivo Data

Animal experiments were reviewed and approved by the Institutional Animal Care and Use Committee (IACUC) at the University of Texas at Dallas. A healthy six-week-old mouse, Charles River Laboratories, Wilmington, MA) was used for our preliminary *in vivo* feasibility test. A 50 µL solution of UCA (Definity, Lantheus Medical Imaging) was diluted to 100 µL with saline and then slowly injected via a winged infusion

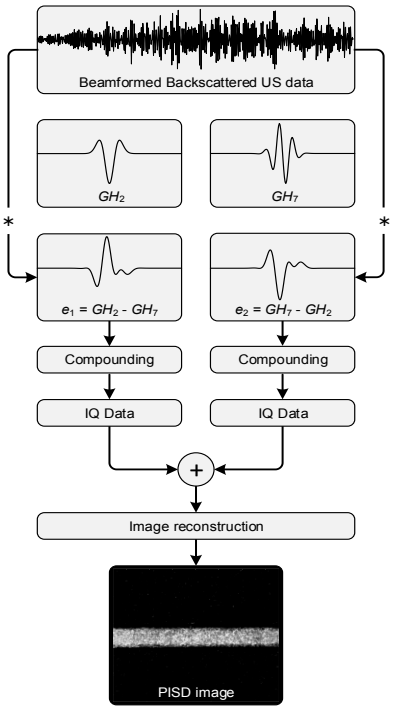

Fig. 1. Schematic diagram of the real-time pulse inversion spectral deconvolution (PISD) method for contrast-enhanced ultrasound (CEUS) imaging. Backscattered ultrasound (US) is acquired and processed using a pair of n^{th}-order Gaussian-weighted Hermite polynomial (GH_n) deconvolution filters after receive beamforming and before any angular compounding and image reconstruction.

catheter (Terumo Corp, Hatagaya, Tokyo, Japan) placed in the tail vein. With the US transducer fixed, PISD and NLI imaging was performed in the hindlimb immediately before and after UCA injection for at least 2 min using MI = 0.2 and N = 9 angles for compounding. During US imaging, the animal was controlled with 2% isoflurane anesthesia (V3000PK, Parkland Scientific, Coral Springs, FL).

E. Statistical analysis

Using a conventional maximum intensity projection (MIP) applied to 250 frames of CEUS data, multiple rectangular region-of-interests (ROIs) were placed to encompass areas perfused with UCA (depth × width = 24 × 100 pixels) or background/tissue (24 × 50 pixels). Using MIP B-mode US image as a reference, a normalized CTR from both PISD and NLI images was calculated from ROI pixels using the formulas:

$$\frac{\left((\mu_{MB}-\mu_T)/\sigma_T\right)_{\mathrm{PISD}}}{\left((\mu_{MB}-\mu_T)/\sigma_T\right)_{\mathrm{PISD_{B-mode}}}} \quad (1)$$

and

$$\frac{\left((\mu_{MB}-\mu_T)/\sigma_T\right)_{\mathrm{NLI}}}{\left((\mu_{MB}-\mu_T)/\sigma_T\right)_{\mathrm{NLI_{B-mode}}}} \quad (2)$$

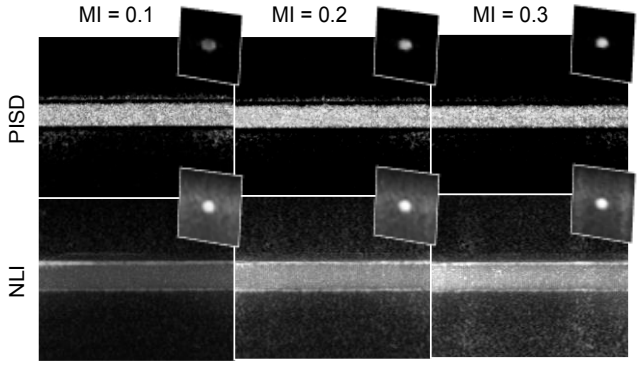

Fig. 2. Representative CEUS images acquired using PISD or nonlinear (NLI) imaging approaches. Images were acquired using an US transmit frequency of 4.5 MHz with variable mechanical index (MI).

where μ and σ denote mean and standard deviation, respectively, and the subscripts *MB* and *T* indicate US image ROIs containing UCA or background signal, respectively.

III. Results and Discussions

PISD is a new CEUS imaging technique that relies on tissue signal suppression and UCA detection during postprocessing of the backscattered US data. This is in difference to the more traditional NLI imaging strategies that rely on multiple transmit pulse sequences that utilize amplitude or phase modulation before summation to detect the MB signal. Detailed in this paper, a series of tissue-mimicking flow phantom studies were conducted and CEUS images were collected in a 4-mm diameter vessel. As illustrated in Fig. 2, both PISD and NLI imaging at 4.5 MHz can be used for UCA detection and visualization of flow. Increasing the MI improves contrast between the MB-filled vessel and background signal from the tissue-mimicking material.

Notwithstanding, use of higher MI values (e.g. greater than 0.5) increases the likelihood of MB destruction during CEUS imaging and will void any quantitative measurements from the data. As above, an improvement in image contrast was noted when performing CEUS imaging at an MI of 0.2 and use of more angles during spatial compounding, Fig. 3.

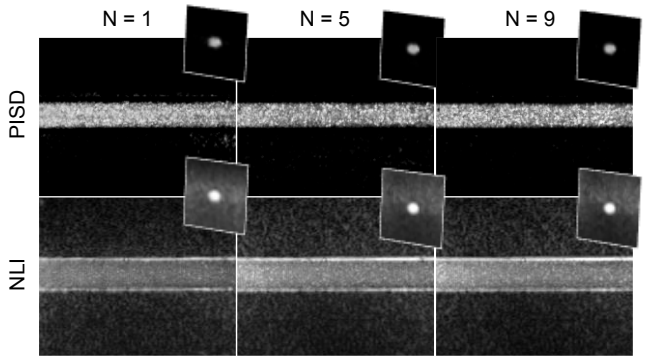

Fig. 3. Representative CEUS images acquired using PISD or NLI approaches. Images were acquired using an US transmit frequency of 4.5 MHz with variable number of steered images *N* used for angular compounding.

TABLE I. Contrast-To-Noise Ratio (CNR) Values (Units, dB) Calculated from PISD and NLI-Based CEUS Imaging As A Function Of MI And Number of Angles Used During Spatial Compounding

Angles	PISD			NLI		
	MI = 0.1	MI = 0.2	MI = 0.3	MI = 0.1	MI = 0.2	MI = 0.3
N = 1	19.0	33.8	47.0	2.3	4.3	7.1
N = 5	24.1	46. 6	56.1	3.6	5.5	6.7
N = 9	30.6	58.8	58.3	4.1	6.1	7.1

As summarized in Table I, CEUS with angular compounding improves CNR measurements. Further, PISD-based CEUS exhibited improved image contrast compared to the NLI imaging approach. Collectively, these results highlight improved image contrast when performing real-time CEUS imaging using PISD and angular compounding at a relatively low MI setting.

Representative *in vivo* CEUS images obtained from a healthy mouse hindlimb are depicted in Fig. 4. These images were collected using an US center frequency of 4.5 MHz and MI of 0.2 with angular compounding (*N* = 9). A MIP was computed from both the PISD and NLI image sequences and presented for comparison. The fine skeletal muscle microvascular detail is clearer in the PISD image compared to the matched NLI. This example illustrates how the PISD-based CEUS imaging approach helps differentiate the MB from tissue signals. Thus, leading to higher image contrast between the microvasculature and the surrounding skeletal muscle tissue. Microvascular structures are poorly visible in the NLI-based CEUS image, which makes any subsequent analysis of vascular morphology or perfusion problematic.

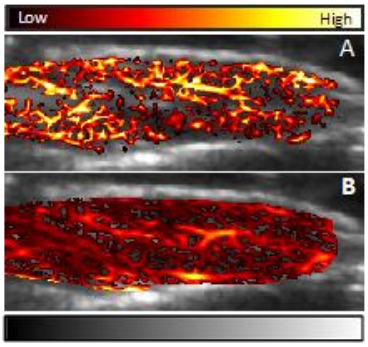

Fig. 4. *In vivo* results in the hindlimb of a healthy mouse after MB injection. Representative CEUS images acquired using (A) PISD or (B) NLI imaging approaches. Images were acquired using an US transmit frequency of 4.5 MHz with MI of 0.2.

IV. Conclusions

PISD is a new signal processing tool to image UCA activity with high sensitivity and spatial specificity. It does not require band-limiting the transmit pulses to simply the separation of the linear and nonlinear signal components. This allows for the use of standard US imaging pulses designed to provide the best

possible resolution while using the full bandwidth of the US imaging transducer. The PISD method detailed herein should not only work on pulse inversion based CEUS imaging approaches, but on all multi-pulse strategies intended to reduce or enhance a specific frequency band.

REFERENCES

[1] S. R. Sirsi and M. A. Borden, "Microbubble compositions, properties and biomedical applications," *Bubble Sci. Eng. Technol.*, vol. 1, no. 1–2, pp. 3–17, 2009.

[2] M. Claudon *et al.*, "Guidelines and good clinical practice recommendations for contrast enhanced ultrasound (CEUS) in the liver – Update 2012," *Ultraschall Med. - Eur. J. Ultrasound*, vol. 34, no. 01, pp. 11–29, 2012.

[3] D. Cosgrove, "Ultrasound contrast agents: An overview," *Contrast Media Mod. Imaging*, vol. 60, no. 3, pp. 324–330, 2006.

[4] P. Sidhu *et al.*, "The EFSUMB guidelines and recommendations for the clinical practice of contrast-enhanced ultrasound (CEUS) in non-hepatic applications: Update 2017," *Ultraschall Med. - Eur. J. Ultrasound*, vol. 39, no. 02, pp. e2–e44, 2018.

[5] R. Saini and K. Hoyt, "Recent developments in dynamic contrast-enhanced ultrasound imaging of tumor angiogenesis," *Imaging Med.*, vol. 6, no. 1, pp. 41–52, 2014.

[6] K. Hoyt, H. Umphrey, M. Lockhart, M. Robbin, and A. Forero-Torres, "Ultrasound imaging of breast tumor perfusion and neovascular morphology," *Ultrasound Med. Biol.*, vol. 41, no. 9, pp. 2292–2302, 2015.

[7] F. Forsberg, W. T. Shi, and B. B. Goldberg, "Subharmonic imaging of contrast agents," *Ultrasonics*, vol. 38, no. 1, pp. 93–98, 2000.

[8] A. Bouakaz, S. Frigstad, F. J. Ten Cate, and N. de Jong, "Super harmonic imaging: a new imaging technique for improved contrast detection," *Ultrasound Med. Biol.*, vol. 28, no. 1, pp. 59–68, 2002.

[9] R. Y. Chiao and Xiaohui Hao, "Coded excitation for diagnostic ultrasound: a system developer's perspective," *IEEE Trans. Ultrason. Ferroelectr. Freq. Control*, vol. 52, no. 2, pp. 160–170, 2005.

[10] P. J. A. Frinking, A. Bouakaz, J. Kirkhorn, F. J. Ten Cate, and N. de Jong, "Ultrasound contrast imaging: current and new potential methods," *Ultrasound Med. Biol.*, vol. 26, no. 6, pp. 965–975, 2000.

[11] D. H. Simpson, Chien Ting Chin, and P. N. Burns, "Pulse inversion Doppler: a new method for detecting nonlinear echoes from microbubble contrast agents," *IEEE Trans. Ultrason. Ferroelectr. Freq. Control*, vol. 46, no. 2, pp. 372–382, 1999.

[12] M. Pasovic *et al.*, "Second harmonic inversion for ultrasound contrast harmonic imaging," *Phys. Med. Biol.*, vol. 56, no. 11, pp. 3163–3180, 2011.

[13] Brock-Fisher GA, Poland MD, Rafter PG., "Means for increasing sensitivity in non-linear ultrasound imaging systems," *US Patent 5*, vol. 577, no. 505, 1996.

[14] R. J. Eckersley, C. T. Chin, and P. N. Burns, "Optimizing phase and amplitude modulation schemes for imaging microbubble contrast agents at low acoustic power," *Ultrasound Med. Biol.*, vol. 31, no. 2, pp. 213–219, 2005.

[15] W. Wilkening, M. Krueger, and H. Ermert, "Phase-coded pulse sequence for non-linear imaging," *Proc IEEE Ultrason Symp*, vol. 2, pp. 1559–1562, 2000.

[16] P. J. Phillips, "Contrast pulse sequences (CPS): imaging nonlinear microbubbles," *Proc IEEE Ultrason Symp*, vol. 2, pp. 1739–1745, 2001.

[17] O. Couture, M. Fink, and M. Tanter, "Ultrasound contrast plane wave imaging," *IEEE Trans. Ultrason. Ferroelectr. Freq. Control*, vol. 59, no. 12, pp. 2676–2683, 2012.

[18] M. Khairalseed, F. Xiong, R. F. Mattrey, K. J. Parker, and K. Hoyt, "Detection of early tumor response to Abraxane using H-scan imaging: Preliminary results in a small animal model of breast cancer," *Proc IEEE Ultrason Symp*, pp. 1–4, 2017.

[19] M. Khairalseed, K. Hoyt, J. Ormachea, A. Terrazas, and K. J. Parker, "H-scan sensitivity to scattering size," *J. Med. Imaging*, vol. 4, no. 4, p. 043501, 2017.

[20] K. J. Parker, "Scattering and reflection identification in H-scan images," *Phys. Med. Biol.*, vol. 61, no. 12, pp. L20-28, 2016.

[21] M. Khairalseed, K. Brown, K. J. Parker, and K. Hoyt, "Real-time H-scan ultrasound imaging using a Verasonics research scanner," *Ultrasonics*, vol. 94, pp. 28–36, 2019.

[22] M. Khairalseed, F. Xiong, J.-W. Kim, R. F. Mattrey, K. J. Parker, and K. Hoyt, "Spatial angular compounding technique for H-scan ultrasound imaging," *Ultrasound Med. Biol.*, vol. 44, no. 1, pp. 267–277, 2018.

[23] H. Tai, M. Khairalseed, and K. Hoyt, "Adaptive attenuation correction during H-scan ultrasound imaging using K-means clustering," *Ultrasonics*, 2019 (published online).